

Emission Zone Measurement Gives Insight into the Suitability of Accelerated Ageing Extrapolation

R. Mac Ciarnáin^{1,2}, H.W. Mo^{3,4}, K. Nagayoshi³, H. Fujimoto^{3,4}, K. Harada^{3,4},
T. H. Ke¹, P. Heremans^{1,2} & C. Adachi⁴

Rossa.MacCiarnain@imec.be

¹IMEC Kapeldreef 75, 3001, Leuven, Belgium

²KU Leuven, Oude Markt 13, 3000 Leuven, Belgium

³³-OPERA, 5-14 Kyudai-shimmachi, Nishi-ku, Fukuoka-shi, 819-0388, Japan

⁴OPERA, Co-Evolutional Social Systems Building #224, 744 Motooka, Nishi, Fukuoka 819-0395, Japan.

Keywords: OLED ageing emission-zone degradation stability

ABSTRACT

Accelerated OLED ageing at higher current densities is commonly used to extrapolate lower current density device lifetime benchmarks. Different emission zones and device ageing were measured at different current densities giving more insight into the suitability of such accelerated ageing assumptions.

1 INTRODUCTION

The T97 or T95 lifetime, or the time taken to reach 97% or 95% luminance via ageing under electrical operation are conventional benchmarks for OLED development. However, it can take months to measure these for state of the art OLEDs. The concept of accelerated ageing at higher current densities was introduced in 2002 by Aziz et al. [1], who assumed a Coulombic degradation mechanism only, as was suggested by Van Slyke et al. in 1996 [2].

This assumption was experimentally tested in 2005 by Féry et al. [3]. They used stretched exponentials to model lifetime curves over a range of luminances (and hence, current densities), fitting the data well. Then it was shown that the stretched exponential coefficient is constant for all curves. It was explained that a single mechanism is responsible for the ageing process at all luminances. Therefore, they concluded that one can accurately predict a lower luminance lifetime from a higher or accelerated ageing lifetime measurement via extrapolation.

Up to today, many publications in high impact journals have referenced and used this accelerated ageing assumption, but for large current density/luminance ranges. For example, 3 mA/cm² and 30 mA/cm² [4], 1000 and 5000 cd/m² [5], 1000 cd/m² and 30 mA/cm² [6] and 100 and 1000 cd/m² [7].

However, in the previously mentioned work by Féry et al. [3] only a small range of luminances, from 100 to 800 cd/m² was used. Perhaps because of the small range, evidence for different degradation mechanisms at different current densities or luminances was not observed. One important related concept is a current density dependent emission zone. The emission zone in an OLED is the volume from where light is emitted via exciton relaxation

[8]. It should depend on current density as it forms from the recombination zone of holes and electrons widened by exciton diffusion [8]. The emission zone has been shown to strongly affect OLED lifetime [7,9,10].

Direct emission zone measurements of OLEDs have proved quite difficult. To the best of our knowledge, only two *direct* experimental measurements of the emission zone in an OLED have been published [8],[11]. Both these two papers feature highly-unexpected interface-dominant emission zones in highly efficient OLEDs. Additionally, these works require a precisely aligned angular spectra measurement setup which is not available to every OLED research lab.

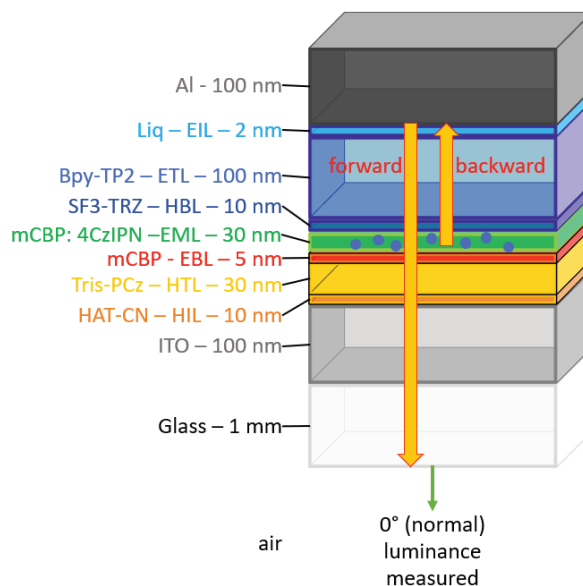


Fig. 1 OLED structure. ETL thickness (~ source-mirror distance) is chosen to give destructive interference between forward and backward waves, giving information on the emission zone. Emitter molecules are sketched as blue circles.

For a standard OLED designed for maximum optical outcoupling, which uses a constructive interference microcavity, small changes in the light source position do not cause visible changes in the emitted spectrum. However, if the OLED source-mirror distance is chosen so that the forward and the backward propagating wave (reflected off the dominant reflective layer - the mirror) destructively interfere (as can be seen in Fig.1), this destructive interference is visible as a dip in the emitted spectrum (see Fig.2). Destructive interference is very sensitive to small changes in the position of the source(s), i.e., a small shift in the position of the source in the microcavity can significantly alter the destructive interference resonance in the far-field emission spectrum. In this way, information on the emission source positions can be extracted [12].

In this work, measurements via a novel application of the microcavity inverse light-outcoupling emission zone method [12], needing only standard JVL measurements at 0° (normal) emission only, will be shown. At 0° emission, perpendicular emitter components are not visible due to the microcavity interference conditions, and so the emitter ensemble average orientation can be neglected in the analysis. Direct experimental measurement of the OLED emission zone over 4 orders of magnitude current density will be presented. Previously, finely aligned multi-angular measurements were used, along with polarization optics, allowing only 1.5 orders of magnitude current density to be measured [11]. Significant changes in the emission zone with current density result and the effect of this on the accelerated ageing assumption will be investigated.

2 EXPERIMENTAL

OLED devices as shown in Fig. 1, were deposited on commercial ITO (Indium tin oxide) anode-on-glass substrates via thermal evaporation under a high vacuum of 10^{-6} torr. A HAT-CN hole injection layer (HIL) was deposited at 0.1 Å/s and an Liq electron injection layer (EIL) at 0.2 Å/s. The EML (emission layer) was co-deposited, with the mCBP host having a rate of $1-x$ Å/s and the 4CzIPN emitter with a rate of x Å/s, where x is the required emitter concentration as a fraction. The hole transport layer (HTL), the electron blocking layer (EBL), the hole blocking layer (HBL), the electron transport layer (ETL) and the Al cathode (in a different chamber) were deposited at a rate of 1 Å/s. Immediately after fabrication, the devices were encapsulated under glass using epoxy glue in a nitrogen-filled glovebox with $H_2O < 0.1$ ppm and $O_2 < 0.1$ ppm. The device active area dimensions were 2 mm x 2 mm. Stack materials were chosen following a published 4Cz-IPN TADF green emitter reference stack [4].

OLED devices were driven at various current densities using a Keithley 2635B source meter and 0° emission spectra (normal to the OLED layer planes) were acquired using a Konica Minolta CS 2000 spectroradiometer.

Optical simulations to compare with the experimentally measured spectra were performed with the commercial software Setfos, version 5.0.1. These simulations used an emission zone model of 10 discrete weighted points, evenly spaced across the EML. A Gaussian function was used to constrain the values of these weighted points. A least squares fit of the simulated to the experimental 0° emission spectra was performed to give the best fitting Gaussian emission zone functions.

3 RESULTS

Simulation to experimental spectrum fitting results (upper parts) along with the resulting extracted emission zone profiles (lower parts) are shown in Fig.2. The red lines in the upper parts represent simulated spectra and the black lines represent the experimentally measured spectra (1 nm sampling). The discrete simulation positions can be observed in the lower parts in green, each having a spacing of 4 nm and an individual variable emission weight. The sum of all emission weights for each device is normalised to 1. The red sections in the lower diagram parts represent the EBL and the blue sections represent the beginning of the HBL. The central white layer in between represents the EML.

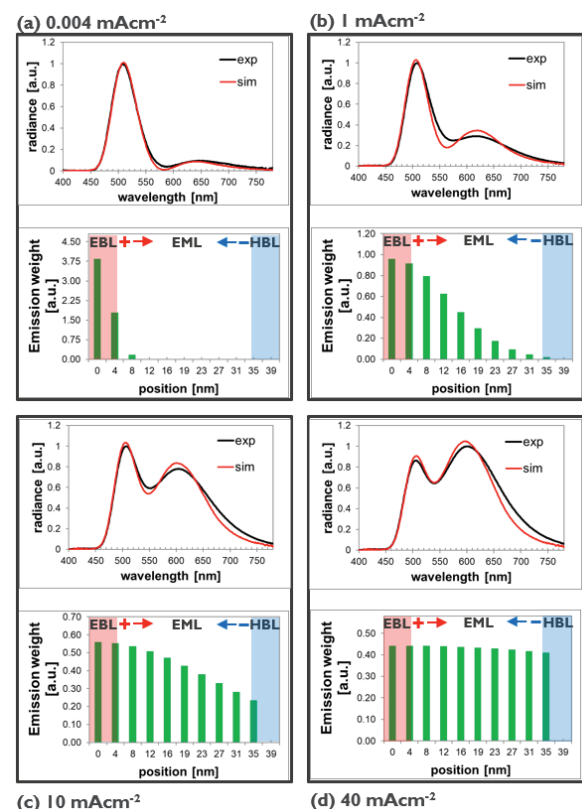


Fig. 2 Simulation to experimental spectrum fitting results (above) with the resulting emission zone profiles extracted (below) for 4 different current densities of a device with 20% emitter doping concentration

Part (a) of Fig. 2. shows data at the device turn on point, 0.004 mAcm^{-2} . Part (b) shows data for 1 mAcm^{-2} , part (c) shows data for 10 mAcm^{-2} and finally, part (d) shows data for 40 mAcm^{-2} . Regarding the simulation boundary conditions, emission was allowed from the EML and EBL. Evidence from experiments (yet unpublished and outside of the scope of this paper) where contamination was applied at the EBL-EML interface in one device and at the HTL-EBL interface in another device showed the same device degradation effect. Since such degradation was found only to occur where the emission zone overlapped with the contamination, this indicates that the emission zone extends to the HTL-EBL interface.

In Fig.3, measured LT95 lifetimes are measured at current densities of 1 mAcm^{-2} , 10 mAcm^{-2} and 40 mAcm^{-2} for devices with emitter concentrations from 10% to 50%. Linear extrapolation from the 10 mAcm^{-2} and 40 mAcm^{-2} data points (which can be relatively quickly measured) is performed to get the 1 mAcm^{-2} LT95 values. These values are then compared with the actual measured values in Table 1.

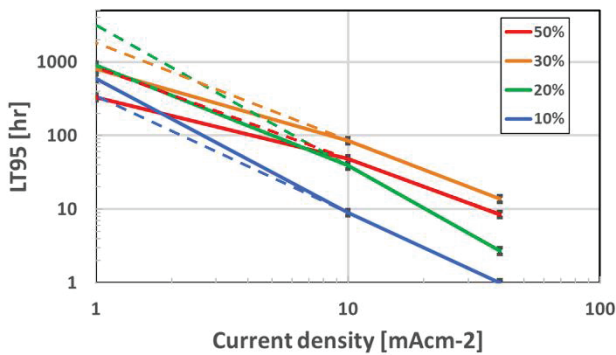


Fig. 3 Log-log graph showing non-linear behavior for devices with various emitter concentrations. Error bars are shown in black for 1 mAcm^{-2} , 10 mAcm^{-2} and 40 mAcm^{-2} data points. Solid lines connect measured data points, dashed lines show extrapolation to 1 mAcm^{-2}

Device	Measured T95 @ 1 mAcm^{-2} [hr]	Extrapolated T95 @ 1 mAcm^{-2} [hr]	% Error
10%	600	370	-38%
20%	900	3000	+233%
30%	800	1900	+138%
50%	330	800	+142%

Table. 1 Percentage error in accelerated ageing extrapolation

4 DISCUSSION

The results in Fig.2, show that, for the lowest current density, the emission zone profile is located at the EBL-EML interface. This indicates that at device turn-on, the electron current dominates in the EML. As the current density is increased, the emission zone profile spreads more and more towards the EML-HBL interface. This indicates that the hole current in the EML increases at a greater rate than the electron current as the current density in the device is increased. At a high current density of 40 mAcm^{-2} , the electron and hole currents in the EML seem quite balanced.

Evidence has been previously shown, for devices which differ only by the HBL material from the devices in this work, that the device lifetime is strongly affected by having different emission zones by varying the concentration of the electron-transporting emitter [13]. A trend with emitter concentration also results here, shown in Table 1. The presence of different degradation mechanisms for different emission zones, and therefore current densities, can explain the non-linear measurement lines (solid lines) in Fig.3. If the accelerated ageing assumption that only a single degradation mechanism was responsible for ageing at all current densities was appropriate for these devices, then the measurement lines would be linear. In this work, errors in the extrapolated lifetime as high as 233% result, showing that the accelerated ageing assumption does not work for these devices.

5 CONCLUSIONS

For the devices in this work, the accelerated ageing assumption and extrapolation method cannot be relied upon. If the accelerated ageing extrapolation is used, errors as high as 233% result. Different degradation effects are evident at different current densities which seems to be caused by a changing emission zone. It is suspected that this is a general trend, at least for TADF OLEDs. The methods of this paper can be easily transferred to a study on fluorescent OLEDs, phosphorescent OLEDs and even Perovskite LEDs.

We appreciate the support of the Japanese government through the innovation ecosystem project in Fukuoka administered by Prof. R. Hayashi of Shibaura Institute of Technology, Tokyo.

REFERENCES

- [1] H. Aziz, Z. D. Popovic, and N. Hu, "Organic light emitting devices with enhanced operational stability at elevated temperatures", *Appl. Phys. Lett.* 81, no. 2, pp. 370–372, (2002).
- [2] S. a. Van Slyke, C. H. Chen, and C. W. Tang, "Organic electroluminescent devices with improved

stability”, *Appl. Phys. Lett.*, 69, no. 15, p. 2160, (1996).

- [3] C. Féry, B. Racine, D. Vaufrey, H. Doyeux, and S. Cinà, “Physical mechanism responsible for the stretched exponential decay behavior of aging organic light-emitting diodes”, *Appl. Phys. Lett.* 87, 213502 (2005).
- [4] M. Tanaka, R. Nagata, H. Nakanotani, & C. Adachi, “Understanding degradation of organic light emitting diodes from magnetic field effects,” *Commun Mater* 1, 18 (2020).
- [5] L.S. Cui, S.B. Ruan, F. Bencheikh, R. Nagata, L. Zhang, K. Inada, H. Nakanotani, L.S. Liao & C. Adachi, “Long-lived efficient delayed fluorescence organic light-emitting diodes using n-type hosts”, *Nat Commun* 8, 2250 (2017).
- [6] T. Kamata, H. Sasabe, N. Ito, Y. Sukegawa, A. Arai, T. Chiba, D. Yokoyama and J. Kido, “Simultaneous realization of high-efficiency, low-drive voltage, and long lifetime TADF OLEDs by multifunctional hole-transporters”, *J. Mater. Chem. C*, 8, 7200, (2020).
- [7] Y. Zhang, J. Lee & S.R. Forrest, “Tenfold increase in the lifetime of blue phosphorescent organic light-emitting diodes”, *Nat. Commun.* 5:5008, (2014).
- [8] R. Mac Ciarnain, D. Michaelis, T. Wehler, A.F. Rausch, N. Danz, A. Bräuer, A. Tünnermann, “Emission from outside of the emission layer in state-of-the-art phosphorescent organic light-emitting diodes”, *Org. El.* Vol. 44, 115-119, (2017).
- [9] R. Meerheim, S. Scholz, S. Olthof, G. Schwartz, S. Reineke, K. Walzer, Karl Leo, “Influence of charge balance and exciton distribution on efficiency and lifetime of phosphorescent organic light-emitting devices”, *J. Appl. Phys.* 104, 014510 (2008).
- [10] S. K. Jeon, J. Y. Lee, “Four times lifetime improvement of blue phosphorescent organic light-emitting diodes by managing recombination zone”, *Org. El.* Vol. 27, 202-206, (2015).
- [11] M. Regnat, K. P. Pernstich, S. Züfle, B. Ruhstaller “Analysis of the Bias-Dependent Split Emission Zone in Phosphorescent OLEDs”, *ACS Applied Materials & Interfaces* 10 (37), 31552-31559 (2018).
- [12] M. Flämmich, D. Michaelis, N. Danz, “Accessing OLED emitter properties by radiation pattern analyses”, *Org. Electron.*, 12 p. 83, (2011).
- [13] H. Nakanotani, K. Masui, J. Nishide, T. Shibata, C. Adachi, “Promising operational stability of high-efficiency organic light-emitting diodes based on thermally activated delayed fluorescence” *Sci Rep* 3, 2127 (2013).